

Korumilli TARANGINI<sup>1\*</sup>, K. JAGAJANANI RAO<sup>1</sup>, Stanisław WACŁAWEK<sup>2</sup>  
Miroslav ČERNÍK<sup>2</sup> and Vinod V.T. PADIL<sup>2\*</sup>

## ***AEGLE MARMELLOS* LEAF EXTRACT BASED SYNTHESIS OF NANOIRON AND NANOIRON+Au PARTICLES FOR DEGRADATION OF METHYLENE BLUE**

**Abstract:** In this study, nanoiron and nanoiron+Au particles were synthesised using aqueous *Aegle marmelos* extract using a facile and one-pot approach. Lower size non-magnetic nanoiron (~34 nm) and nanoiron (~34 nm) +Au particles (1 to 1.5 μm) were produced from the same medium individually. Nanoparticles suspension behaviour and structural characterisations were carried out by UV-Vis spectroscopy, electron microscopy and by X-ray diffraction techniques. Primarily, for synthesis, a simple bioreduction approach generated amorphous nanoiron particles, which on annealing produced magnetic maghemite,  $\gamma$ -Fe<sub>2</sub>O<sub>3</sub> type nanoparticles with sizes 100 to 1000 nm. Posteriorly, the bioreduction process also produces nanoiron+Au particles and can be used for multifunctional applications. As a model application, catalytic application of the as-prepared nanoiron and nanoiron+Au particles towards methylene blue, a thiazine dye degradation is investigated and found to be effective within 20 min. Langmuir-Hinshelwood kinetic model was exploited to know the degradation behaviour, and the model was found to be fit based on  $R^2$  values with the observed experimental data. We suggest that the formed highly stable nanoiron particles with *in situ* stabilisation offer benefits like consistency, environmental friendliness and suits well for large-scale applicability.

**Keywords:** nanoiron, gold plates, methylene blue, maghemite, bioreduction, *Aegle marmelos*

### **Introduction**

In the current scenario, nanoparticles through green synthesis approaches had been considered a more environmentally beneficial, safer and cost-effective alternative to existing physical and chemical methods [1-4]. Plant biomolecules are promising sources for green production of a variety of nanomaterials and these approaches possess advantages like freely available, non-toxic, inexpensive, offer simplicity of use and scalability [2, 5-7]. Extracts from plant sources contain key molecules like antioxidants, polyphenols, nitrogenous bases, reducing sugars, amino acids and redox chemicals which are capable to reduce metal ions and metal salt solution [1, 8, 9]. Particle formation from plant extracts involves the formation of nucleation centres, sequestering with additional metal ions and eventually leads to the formation of nanoparticles [1, 8-10]. Organic molecules from plant

<sup>1</sup> Department of Biotechnology, Vel Tech Rangarajan Dr. Sagunthala R&D Institute of Science and Technology, Chennai-600062, India, email: drktrarangini@veltech.edu.in, ORCID: KT 0000-0003-0678-8903

<sup>2</sup> Department of Nanomaterials in Natural Sciences, Institute for Nanomaterials, Advanced Technologies and Innovation (CXI), Technical University of Liberec (TUL), Studentská 1402/2, Liberec 1 461 17, Czech Republic, ORCID: VVTP 0000-0002-0816-526X, SW 0000-0002-8430-8269, MC 0000-0002-7554-020X

\* Corresponding author: vinod.padil@tul.cz

sources serve to improve particle stability through *in situ* capping, and many reported methods demonstrate no toxicity compared with conventional chemical methods [10-12].

Although there are many reported studies, showing the production of silver and gold particles using various routine to specific plant extracts from *Aloe vera* [9], hibiscus [6, 8], black tea [13], coffee [14], sorghum [5] fruit extracts [15] and tree gums [16], efficient synthesis of iron nanoparticles through methodologies is not merely simple and is subsequently occasionally reported. This is because reduced iron is more prone to oxidation in solution than compared to gold and silver particles leading to greater particle instability [17]. Although nanoiron particles are more reactive; particle agglomeration, broad size distributions and stringent reaction conditions are common difficulties associated with their production techniques [17-19]. However, some studies reported amorphous or zerovalent Fe nanoparticles that can be synthesised using extracts and molecules such as tea [20], coffee, sorghum, tannins [21] and others [17, 22]. In these studies, nanoiron particles of various sizes and shapes can be produced instantaneously in aqueous media, and reports demonstrated their use in the degradation of organic contaminants effectively. Nanoparticles synthesis from biochemicals like tannins have particular advantages like natural, non-toxic, abundantly available in plant materials (like leaves, fruits, wood, bark) contains biodegradable polyphenolic compounds and easily extractable from plant sources [20, 21, 23, 24]. These have the ability to form ready complexes with iron and other metallic cations [20, 23, 24].

Based on our reported studies, tannins from *Aegle marmelos* leaf extract (LE) can produce nanoparticles like silver and gold [2, 23, 24]. Here, hydrolysable tannins like procatechuic acid type molecules were identified as key agents responsible for *in situ* synthesis and stabilisation effect. In order to elucidate the role of LE tannins in synthesising iron nanoparticles, we decided to work with LE tannins with mild modification of the process parameters. Though the production of nanoiron particles employing various plant extracts has been reported [17, 22]; technology and approach to producing stable particles with controlled size and morphology are still of main interest. Readymade iron nanoparticles applied with limited purification steps towards favourable large-scale environmental remediation and hazardous waste treatment applications are of particular interest [17, 20, 21, 25]. In this work, we characterised the formation of iron nanoparticles using aqueous LE extract and demonstrated the potential of the same extract to produce plate type Au nanoparticles with amorphous nanoiron particles combined. Furthermore, the annealing approach to produce magnetic iron nanoparticles was investigated, and the ability of the as-synthesised nanoiron and nanoiron+Au particles towards methylene blue (MB) degradation was evaluated. Here, MB dye was selected as a model dye as it is widely used in textile dyeing and is very much toxic and carcinogenic upon release into the nearby aquatic environment [10, 17, 26].

## Materials and methods

The use of *Aegle marmelos* extract (LE) for nanoiron particle synthesis is the primary step in this study. Aqueous LE was prepared in powder form primarily according to the procedure detailed in our earlier study [23]. To 10 mL of 5 % LE solution, 10 mL of phosphate buffer solution and 2 mL of 0.1 M NaOH solution was added and sonicated for 15 min. After 10 min, the resultant LE was centrifuged at 5000 rpm for 20 min; the supernatant was collected and stored. To 1 mL of this treated LE solution, which is having

a pH of  $\sim 10.4$ ; 100  $\mu\text{L}$  of  $\text{Fe}(\text{NO}_3)_3 \cdot 9\text{H}_2\text{O}$  (from 150 mM) was added and subjected to probe sonication for 2 min (pulse on - 10 s and pulse off - 5 s) at room temperature, i.e.  $27 \pm 1$   $^\circ\text{C}$ . The colour change of the solution changed to peanut brown colour indicating the formation of nanoiron particles. In order to make the formed particles magnetic, the resulted particle suspension was exposed to 600  $^\circ\text{C}$  for 1 h in a furnace using a ceramic holder with a temperature increment of 18  $^\circ\text{C}/\text{min}$ . Annealed and as-prepared nanoparticles were subjected to further investigations.

LE's ability to produce simultaneous nanoiron and nanoiron+Au particles was also investigated and observed. Here, to 1 mL of treated LE solution,  $\text{Fe}(\text{NO}_3)_3 \cdot 9\text{H}_2\text{O}$  and  $\text{HAuCl}_4$  were simultaneous added, mixed and subjected to probe sonication as stated above. The colour of the solution turned brown with visible scintillations from particles in the suspension. Here, the concentration of metal salts used was 13.27 mM each for the synthesis process.

MB degradation activity was studied using nanoiron and nanoiron+Au particle suspensions individually at 25  $^\circ\text{C}$  and with 150 rpm. Typically, 20  $\mu\text{M}$  of dye was exposed to 0.53 mg/mL nanoparticle catalysts of each type and with 15  $\mu\text{M}$  borohydride solution. The working volume used for the investigation was 10 mL and nanoparticle suspensions were allowed to equilibrate for 3 min before adding dye. Here, pH of the solution was adjusted to 4 prior experimentation, and with no significant depletion of UV-Vis spectrum of MB, the borohydride solution was then added. The concentration of MB was measured using UV-Vis spectroscopy, and the residual amount estimated through the absorption maximum of the dye at 660 nm.

UV-Vis spectra of the samples were observed using Cyberlab UV100, UV-Vis spectrophotometer. The scanning electron microscopy (SEM) observations were performed on JEOL-2100F, India machine. Field emission scanning electron microscope (FESEM) measurements along with energy-dispersive X-ray spectroscopy (EDX) were done using Carl Zeiss, Neon 40, India instrument. X-ray diffraction (XRD) measurements were done by Philips X-ray diffractometer (PW1830 HT, India) with an accelerating voltage of 35 kV, with a current of 30 mA. The muffle furnace used for the study was from Everflow Scientific Instruments, India. Centrifugation of nanoparticle suspensions was performed using Remi PR24, Remi Lab, India. Unless otherwise stated, all the chemicals used in this study are purchased from Sisco Research Laboratories, India and Ultrapure water with 18.2  $\text{m}\Omega \cdot \text{cm}$  resistivity was used throughout the study. Further, all the investigations were done in triplicate and average values are reported.

## Results and discussion

*Aegle marmelos* leaf extract (LE) rich in polyphenols, especially tannins (capable of reducing metal salts such as Ag and Au) was selected based on our previous reports [2, 23, 24]. We hypothesise that they are able to synthesise iron nanoparticles usually magnetite/maghemite [27]. Considering that nanoiron synthesis was reported by various research groups at alkaline conditions; LE is maintained at pH value of  $\sim 10$  and at ambient room temperature ( $\sim 27$   $^\circ\text{C}$ ) for the bioreduction process. Figure 1a shows the UV-Vis absorption spectrum from nanoiron suspension (within 15 min of addition of iron precursor). The maximum spectral absorption of this suspension was found to be at 470 nm and this optical signal is due to the surface plasmon resonance absorbance of the tannin capped nanoiron particles in the medium. A relatively narrow absorption spectrum between

the wavelength range of 400 to 650 nm indicates that the formed nanoparticles are more symmetric [28]. Supporting the spectral behaviour of nanoiron sols, Figure 1b shows FESEM images of the as-prepared particles using LE, and their average particle size was found to be  $34 \pm 7$  nm. The powder sample (obtained by centrifugation at 18000 rpm for 20 min, followed by washing and drying steps) was subjected to XRD analysis to know the crystalline structure and its diffraction pattern is shown in Figure 1c. With no significant XRD peaks, our sample has an intensity similar to the amorphous type nanoiron particles. This indicates ferroferric oxide or ferric oxide type amorphous nanoparticles as reported by some research groups [18, 29]. As our synthesis process involves the ultrasonication step, there is a consistent possibility of atomic-level mixing, facilitating the favourable formation of the amorphous phase as shown in reported studies [18, 29] and is consistent with our result (Fig. 1c).

Additionally, the formed nanoiron particles exposed to a high-temperature annealing process at 600 °C and transformed into magnetic nanoparticles, as shown in Figure 2. Reports state that high temperatures will influence the size of the particles *via* the sintering effect and larger size nanoiron structures are evident on SEM analysis of the annealed particulate suspension (Fig. 2a,b). Further analysis by TEM displayed the nanoiron particles at this stage are from 100 to 500 nm with varying sizes and shapes (Fig. 2c). XRD analysis of annealed nanoiron particles is shown in Figure 2 which reveals that the diffraction pattern formed is close to maghemite,  $\gamma$ -Fe<sub>2</sub>O<sub>3</sub> phase (JCPDS:04-0755) and infers the formed particles are crystalline in nature.

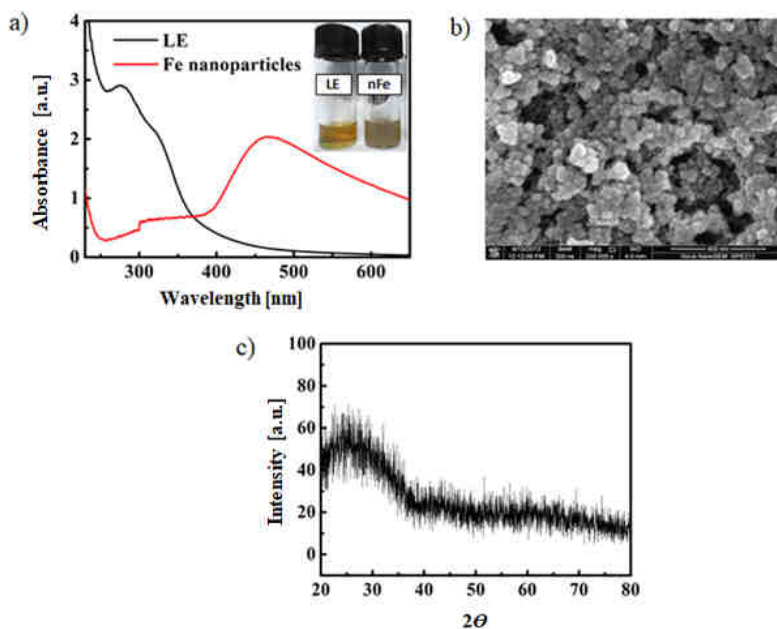


Fig. 1. a) UV-Vis spectra of nanoiron particles suspension and LE, b) corresponds to FESEM images and c) is XRD spectrum of the as-prepared nanoiron particles

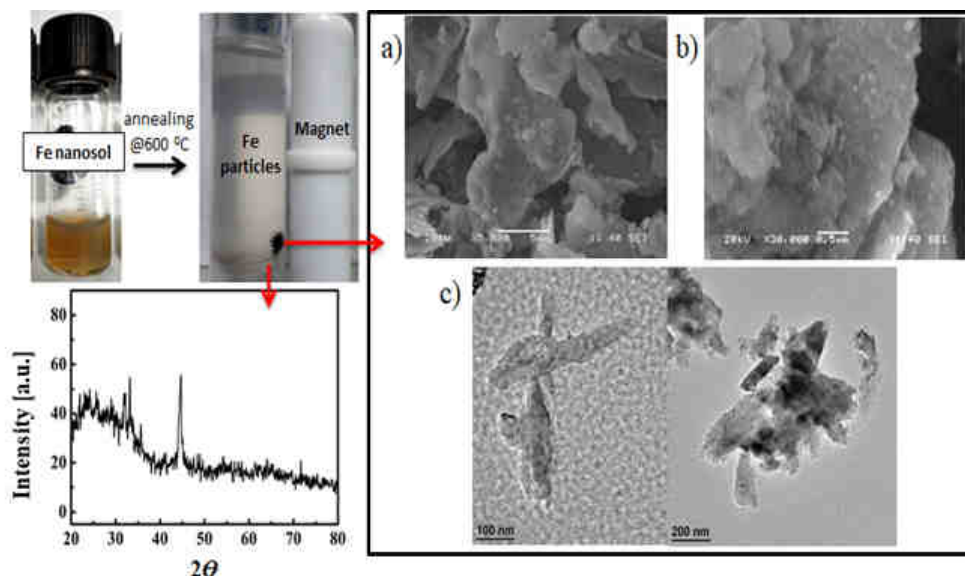


Fig. 2. Nanoiron particle suspension before annealing (picture insert) produced nanoiron particles that exhibit magnetic property when kept near to a bar magnet; a),b) the XRD pattern was given along with SEM and c) TEM images. The magnetic particles from (a-c) display larger sizes with assorted shapes and sizes

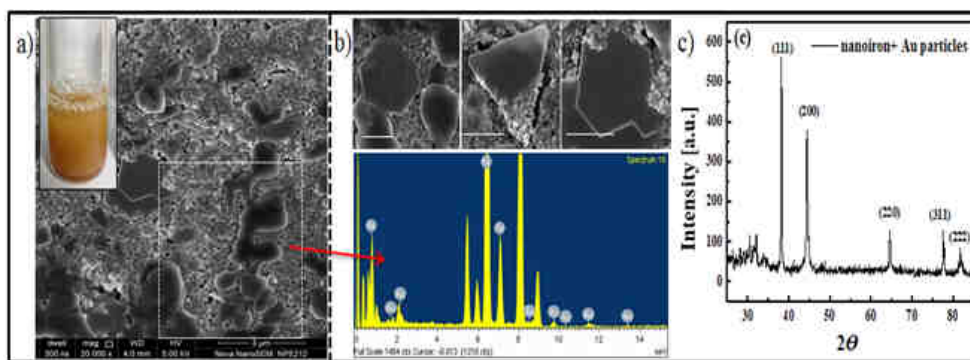


Fig. 3. Particle suspension of nanoiron + Au particles (picture insert of a)), FESEM images (a-b) of the suspension from low to high magnifications and EDX analysis from the selected area of a) and XRD pattern from the powdered particle suspension. Scale bar of SEM images in b) are 1  $\mu$ m

Furthermore, LE was reported to produce nanoAu and reported in our previous study. For further insights regarding the multimetal reduction ability of LE, Au salt was added to the reaction medium, and the morphology of the nanoparticles was observed. Figure 3 shows the formation of nanoiron+Au particles when equimolar concentrations of iron and gold precursors exposed to LE. Particle suspension here produces scintillations in the medium (Fig. 3a, picture insert). As nanoiron has no scintillation effect (Fig. 1a, picture insert), we believe that the observed behaviour is due to Au nanoparticles. FESEM images of the produced articles display nanoiron particles as that of Figure 1b and plate type Au

structures with varied morphologies (hexagons, triangles semi-hexagonal, agglomerated semi-spherical structures) of sizes range from (1 to 1.5  $\mu\text{m}$ ) as shown in Figure 3a,b. The presence of Au and Fe are confirmed through EDX analysis from an area selected from Figure 3a, and XRD pattern from these particles confirmed the crystallinity of Au with face-centered-cubic(fcc) structure matching with JCPDS file no: 04-0784. Here, nanoiron particles in nanoiron+Au particles suspension did not display any diffraction pattern and stood as amorphous as that of sample similar to as-prepared nanoiron particles alone (Fig. 1c). These Au plate type structures in nanoiron+Au particles suspension can be easily separated using 0.4  $\mu\text{m}$  filter (not shown here) and can be used for other special applications.

Detailing MB degradation study, MB removal activity by nanoiron and nanoiron+Au suspensions are evaluated by measuring depleting UV-Vis spectrum of the dye as shown in Figure a,b. It was found that MB concentration decreased significantly with the increase of exposure time with nanoparticles. The results suggest that more than 76 % degradation of MB was achieved in 18 min with both nanoiron and nanoiron+Au particles studied. Nanoiron+Au suspension exhibited no significant enhancement in MB degradation ability when compared to nanoiron particles. This behaviour may attribute to larger sizes of Au particles in nanoiron+Au suspension, and nanoparticles with bigger sizes are catalytically weak in their activity. In addition, the observed MB data (Fig. 4) was enumerated with Langmuir-Hinshelwood equation [30] which is expressed as follows:

$$\ln \frac{A}{A_0} = -kt \quad (1)$$

where  $A$ ,  $A_0$  are final and initial absorbance values of MB at 660 nm,  $k$  is the first-order degradation rate constant and  $t$  is the exposure time. The above equation is a first order rate equation for the degradation process, and measured values displayed a good correlation with  $R^2$  values of  $> \sim 0.98$  for the studied nanoparticle suspensions (Fig. 4c).

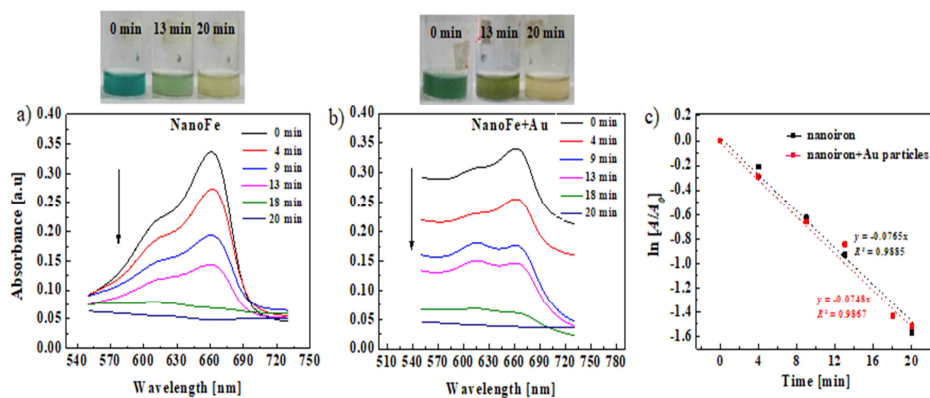


Fig. 4. UV-Vis spectra of MB degradation upon exposure to a) nanoiron and b) nanoiron+Au particle suspensions. Rate constant deduction for a) and b) are shown in c) using Langmuir-Hinshelwood model equation

The degradation activity of the nanoparticle suspensions at ambient light with a decent MB to nanoparticle dose ratio has considerable scope for large-scale applicability. Further,

the net activity can be accelerated upon UV light irradiation as reported in various studies [10, 17]. Smaller nanoiron particles, due to their large surface-to-volume ratio, display superior catalytic activity in acidic environments as evidenced by reported studies (such as degradation of dyes bromothymol blue, methylene orange, methylene blue and monochlorobenzene) [10, 17, 22]. In addition, nanoiron particles easily donate electrons to more electronegative atoms such as chlorine and can be beneficial in treating most organic pollutants [25]. Facile synthesis of stable nanoiron particles in this study has wide spread applicability in ground water treatment, food packing and biomedical fields which are subjects of our future research activities.

## Conclusion

In conclusion, this study investigated the ability of LE to synthesise smaller size stable nanoiron particles from iron salt and we have demonstrated that the as-prepared nanoiron structures can be annealed to attain larger size magnetic particles. Furthermore, the reducing capability of LE was presented with the simultaneous synthesis of nanoiron+Au particles in the same aqueous reaction medium at ambient conditions. Thus, this study offers a rapid, one-pot and facile synthesis approach, which is a safe and attractive option for large scale environmental uses. As a model application, MB degradation was performed using the synthesised nanoiron particles as catalysts and found to be effective within 20 min of exposure times.

## Acknowledgements

The authors would like to thank the University Innovation Cluster-Biotechnology, University of Rajasthan, Jaipur, India for their analysis and characterization support during project execution.

## References

- [1] Nikolaidis P. Analysis of Green Methods to Synthesize Nanomaterials. Green Synthesis of Nanomaterials for Bioenergy Applications. John Wiley Sons, Ltd; 2020. p. 125-44. DOI: 10.1002/9781119576785.ch5.
- [2] Rao KJ, Paria S. *Aegle marmelos* leaf extract and plant surfactants mediated green synthesis of Au and Ag nanoparticles by optimizing process parameters using Taguchi method. ACS Sust Chem Eng 2015. DOI: 10.1021/acssuschemeng.5b00022.
- [3] Wu C-H, Tsai S-B, Liu W, Shao X-F, Sun R, Waclawek M. Eco-technology and eco-innovation for green sustainable growth. Ecol Chem Eng S. 2021;28:7-10. DOI: 10.2478/eces-2021-0001.
- [4] Cepoi L, Zinicovscaia I, Chiriac T, Rudi L, Yushin N, Miscu V. Silver and gold ions recovery from batch systems using biomass. Ecol Chem Eng S. 2019;26:229-40. DOI: 10.1515/eces-2019-0029.
- [5] Njagi EC, Huang H, Stafford L, Genuino H, Galindo HM, Collins JB, et al. Biosynthesis of iron and silver nanoparticles at room temperature using aqueous sorghum bran extracts. Langmuir. 2011;27:264-71. DOI: 10.1021/la103190n.
- [6] Talebpour F, Ghahghaei A. Effect of green synthesis of gold nanoparticles (AuNPs) from *Hibiscus sabdariffa* on the aggregation of  $\alpha$ -Lactalbumin. Int J Pept Res Ther. 2020;26:2297-306. DOI: 10.1007/s10989-020-10023-9.
- [7] Sharifi-Rad M, Pohl P, Epifano F, Álvarez-Suarez JM. Green synthesis of silver nanoparticles using *Astragalus tribuloides* Delile. Root extract: Characterization, antioxidant, antibacterial, and anti-inflammatory activities. Nanomaterials. 2020;10:2383. DOI: 10.3390/nano10122383.
- [8] Alawfi AA, Henari FZ, Younis A, Manaa H. Bio-inspired synthesis of silver nanoparticles using *Hibiscus Tiliaceus* L. flower extracts for improved optical characteristics. J Mater Sci: Mater Electron. 2020. DOI: 10.1007/s10854-020-04619-6

- [9] Kamala Nalini SP, Vijayaraghavan K. Green synthesis of silver and gold nanoparticles using aloe vera gel and determining its antimicrobial properties on nanoparticle impregnated cotton fabric. *J Nanotechnol Res*. 2020;2:42-50. DOI: 10.26502/jnr.2688-85210015.
- [10] Makarov VV, Makarova SS, Love AJ, Sinitsyna OV, Dudnik AO, Yaminsky IV, et al. Biosynthesis of stable iron oxide nanoparticles in aqueous extracts of *Hordeum vulgare* and *Rumex acetosa* plants. *Langmuir*. 2014;30:5982-8. DOI: 10.1021/la5011924.
- [11] Makarov VV, Love AJ, Sinitsyna OV, Makarova SS, Yaminsky IV, Taliansky ME, et al. "Green" nanotechnologies: synthesis of metal nanoparticles using plants. *Acta Naturae*. 2014;6:35-44. Available from: <https://www.ncbi.nlm.nih.gov/pmc/articles/PMC3999464/>.
- [12] Masarovičová E, Kráľová K. Metal nanoparticles and plants. *Ecol Chem Eng S*. 2013;20:9-22. DOI: 10.2478/eces-2013-0001.
- [13] Begum NA, Mondal S, Basu S, Laskar RA, Mandal D. Biogenic synthesis of Au and Ag nanoparticles using aqueous solutions of Black Tea leaf extracts. *Colloids Surfaces B: Biointerfaces*. 2009;71:113-8. DOI: 10.1016/j.colsurfb.2009.01.012.
- [14] Keijok WJ, Pereira RHA, Alvarez LAC, Prado AR, da Silva AR, Ribeiro J, et al. Controlled biosynthesis of gold nanoparticles with *Coffea arabica* using factorial design. *Sci Reports*. 2019;9:16019. DOI: 10.1038/s41598-019-52496-9.
- [15] Doan V-D, Thieu AT, Nguyen T-D, Nguyen V-C, Cao X-T, Nguyen TL-H, et al. Biosynthesis of gold nanoparticles using *Litsea cubeba* fruit extract for catalytic reduction of 4-nitrophenol. *J Nanomaterials*. 2020;2020:10. DOI: 10.1155/2020/4548790.
- [16] Padil VVT, Wacławek S, Černík M. Green synthesis: Nanoparticles and nanofibres based on tree gums for environmental applications. *Ecol Chem Eng S*. 2016;23:533-57. DOI: 10.1515/eces-2016-0038.
- [17] Ali A, Zafar H, Zia M, ul Haq I, Phull AR, Ali JS, et al. Synthesis, characterization, applications, and challenges of iron oxide nanoparticles. *Nanotechnol Sci Appl*. 2016;9:49-67. DOI: 10.2147/NSA.S99986.
- [18] Wang Z, Zhao L, Yang P, Lv Z, Sun H, Jiang Q. Water-soluble amorphous iron oxide nanoparticles synthesized by a quickly pestling and nontoxic method at room temperature as MRI contrast agents. *Chem Eng J*. 2014;235:231-5. DOI: 10.1016/j.cej.2013.09.042.
- [19] Pavelková A, Stejskal V, Vološčuková O, Nosek J. Cost-effective remediation using microscale ZVI: Comparison of commercially available products. *Ecol Chem Eng S*. 2020;27:211-24. DOI: 10.2478/eces-2020-0014.
- [20] Wu Z, Su X, Lin Z, Khan NI, Owens G, Chen Z. Removal of As(V) by iron-based nanoparticles synthesized via the complexation of biomolecules in green tea extracts and an iron salt. *Sci Total Environ*. 2020;142883. DOI: 10.1016/j.scitotenv.2020.142883.
- [21] Herrera-Becerra R, Rius JL, Zorrilla C. Tannin biosynthesis of iron oxide nanoparticles. *Appl Phys A*. 2010;100:453-9. DOI: 10.1007/s00339-010-5903-x.
- [22] Bibi I, Nazar N, Ata S, Sultan M, Ali A, Abbas A, et al. Green synthesis of iron oxide nanoparticles using pomegranate seeds extract and photocatalytic activity evaluation for the degradation of textile dye. *J Materials Res Technol*. 2019;8:6115-24. DOI: 10.1016/j.jmrt.2019.10.006.
- [23] Jagajjanani Rao K, Paria S. Green synthesis of silver nanoparticles from aqueous *Aegle marmelos* leaf extract. *Materials Res Bull*. 2013;48:628-34. DOI: 10.1016/j.materresbull.2012.11.035.
- [24] Rao KJ, Paria S. Green synthesis of gold nanoparticles using aqueous *Aegle marmelos* leaf extract and its application for thiamine detection. *RSC Adv*. 2014;2:28645-52. DOI: 10.1039/C4RA03883E.
- [25] Saleem H, Zaidi SJ. Recent developments in the application of nanomaterials in agroecosystems. *Nanomaterials*. 2020;10:2411. DOI: 10.3390/nano10122411.
- [26] Lellou S, Kadi S, Guemou L, Schott J, Benhebal H. Study of methylene blue adsorption by modified kaolinite by dimethyl sulfoxide. *Ecol Chem Eng S*. 2020;27:225-39. DOI: 10.2478/eces-2020-0015.
- [27] Liu M, Huang R, Che M, Su R, Qi W, He Z. Tannic acid-assisted fabrication of Fe-Pd nanoparticles for stable rapid dechlorination of two organochlorides. *Chem Eng J*. 2018;352:716-21. DOI: 10.1016/j.cej.2018.07.070.
- [28] Herrera-Becerra R, Rius JL, Zorrilla C. Tannin biosynthesis of iron oxide nanoparticles. *Appl Phys A*. 2010;100:453-9. DOI: 10.1007/s00339-010-5903-x.
- [29] Yadav VK, Ali D, Khan SH, Gnanamoorthy G, Choudhary N, Yadav KK, et al. Synthesis and characterization of amorphous iron oxide nanoparticles by the sonochemical method and their application for the remediation of heavy metals from wastewater. *Nanomaterials*. 2020;10:1551. DOI: 10.3390/nano10081551.
- [30] León ER, Rodríguez EL, Beas CR, Plascencia-Villa G, Palomares RAI. Study of methylene blue degradation by gold nanoparticles synthesized within natural zeolites. *J Nanomaterials*. 2016;2016:10. DOI: 10.1155/2016/9541683.